Design and Performance of a Sideband Separating SIS Mixer for 800–950 GHz

Andrey Khudchenko ⑩, Ronald Hesper ⑩, Andrey M. Baryshev, Jan Barkhof, Kirill Rudakov, Daniel Montofré ⑩, Duc van Nguyen, Valery P. Koshelets ⑩, Pavel N. Dmitriev, Michael Fominsky ⑩, Christopher Heiter, Stefan Heyminck, Rolf Güsten, and Bernd Klein

***Abstract*—We present the design and results of characterization of a new sideband separating (2SB) mixer for 800–950 GHz, based on superconductor–insulator–superconductor (SIS) junctions. This is the first waveguide 2SB SIS mixer demonstrated at such a high frequency. The design is following the classical quadrature hybrid architecture, meanwhile additional attention was put on the reduction of reflections in the RF structure in order to minimize the RF imbalance, to achieve a high image rejection ratio (IRR). The RF waveguide block was manufactured by micromilling and populated by single-ended SIS mixers developed earlier for upgrade of the CHAMP+ high-band array on the APEX telescope. These SIS mixers have double-sideband (DSB) noise temperatures from 210 to 400 K. The assembled 2SB mixer yields a SSB noise temperature from 450 to 900 K, with an IRR above 15 dB in 95% of the band. Comparing the DSB and the SSB sensitivities, we find that the waveguide losses are as low as expected and do not exceed 0.6 dB. The presented mixer is a prototype for use in a 2SB dual polarization receiver planned for deployment on the APEX telescope.**

***Index Terms*—Image rejection ratio (IRR), sideband separating (2SB) mixers, submillimeter wave technology, superconductor–insulator–superconductor (SIS) junctions, terahertz receivers.**

A. Khudchenko is with the Kapteyn Astronomical Institute, University of Groningen, 9747 AD Groningen , The Netherlands and also with the Kotel'nikov Institute of Radioengineering and Electronics RAS, 125009 Moscow, Russia (e-mail: a.khudchenko@sron.nl).

R. Hesper, A. M. Baryshev, and J. Barkhof are with the Kapteyn Astronomical Institute, University of Groningen, 9747 AD Groningen, The Netherlands (e-mail: r.hesper@astro.rug.nl; a.m.baryshev@astro.rug.nl; j.barkhof@sron.nl).

K. Rudakov is with the Kapteyn Astronomical Institute, University of Groningen, 9747 AD Groningen, The Netherlands, and with the Kotel'nikov Institute of Radioengineering and Electronics RAS, 125009 Moscow, Russia, and also with the Moscow Institute of Physics and Technology, 141700 Moscow, Russia (e-mail: k.rudakov@astro.rug.nl).

D. Montofré is with the Kapteyn Astronomical Institute, University of Groningen, 9747 AD Groningen, The Netherlands, and also with the Electrical Engineering Department, Universidad de Chile, Santiago 8320000, Chile (e-mail: danielmontofre@gmail.com).

D. van Nguyen is with the Netherlands Institute for Space Research, 9747 AD Groningen, The Netherlands (e-mail: d.van.nguyen@sron.nl).

V. P. Koshelets, P. N. Dmitriev, and M. Fominsky are with the Kotel'nikov Institute of Radioengineering and Electronics RAS, 125009 Moscow, Russia (e-mail: valery@hitech.cplire.ru; pavel@hitech.cplire.ru; ffke@yandex.ru).

C. Heiter, S. Heyminck, R. Güsten, and B. Klein are with the Max Planck Institute for Radio Astronomy D-53121 Bonn, Germany (e-mail: cheiter@mpifr-bonn.mpg.de; heyminck@mpifr-bonn.mpg.de; rguesten@mpifr-bonn.mpg.de; bklein@mpifr-bonn.mpg.de).

Color versions of one or more of the figures in this article are available online at http://ieeexplore.ieee.org.

Digital Object Identifier 10.1109/TTHZ.2019.2939003

I. INTRODUCTION

GROUND-BASED observations of astronomical objects at very high radio frequencies, say a few hundred gigahertz, get progressively more and more compromised with rising frequency due to absorption in the atmosphere. Because a large part of this absorption can be attributed to water vapor, telescopes intended for this part of the spectrum are situated in high and especially dry locations. However, with frequencies approaching 1 THz, even in these places the limiting factor tends to be the atmosphere. Apart from taking the observations to space or stratospheric platforms, which each have severe limitations by themselves, one mitigating technology that has proven its worth at slightly lower frequencies is the employment of sideband-separating (2SB) receivers. Up to recently, this type of receiver was deployed in actual observatories for frequencies up to about 500 GHz [1], while the highest bands in ground-based observatories are still populated with double-sideband (DSB) receivers [2]. In this article, we extend the range of viable sideband-separating receivers to the 800–950 GHz band, which corresponds to the highest atmospheric window where practical observations can be performed.

Using sideband-separating receivers instead of DSB ones allows us to reduce the atmospheric noise contribution for spectral line sources by, ideally, a factor of two, irrespective of the actual atmospheric transparency. In practice, however, the total system noise temperature includes other contributions like mixer noise and intermediate frequency (IF) amplifier noise. These make a factor of two improvement in system noise temperature unobtainable. In addition, the actual improvement will strongly depend on the atmospheric transparency. From historical weather conditions at the APEX [3] and ALMA [4] sites [5], the zenith atmospheric transmission for the 800–950 GHz window can be estimated between 0.2 and 0.6. The atmospheric transparency in these locations is within this range up to 40% of the available time [6]. The upper limit corresponds to realistic good weather conditions, while the bottom is the limit at which the atmospheric opacity becomes too high for reasonable observations in this

band. Within this range, the ratio of the 2SB and DSB sensitivities for spectral line observations will on average be around 1.3 for an effective atmospheric temperature of 260 K, and a state-of-the-art DSB mixer noise temperature of about 150 K [7], [8]. This number gives sufficient motivation to develop 2SB receivers for this frequency range. Note that this gain in sensitivity is only valid for spectral line observations, in both single dish and interferometer modes. However, for continuum sources this number is reduced by another factor of $\sqrt{2}$ in case of an interferometer and 2 for a single dish telescope [9], [10].

Building 2SB mixers for these high frequencies is a challenging task due to the required miniaturization of the waveguide structures. A large step forward was the demonstration of a balanced SIS 787–950 GHz mixer [11]. Nevertheless, up to now, the highest frequency band covered by a 2SB waveguide receiver based on SIS junctions was the atmospheric window of 600–720 GHz [12]. The mixer described in this reference is installed in the SEPIA660 receiver on APEX, and was commissioned in November 2018. It demonstrates very high image rejection ratio (IRR), improved sensitivity and extended frequency range allowing ground-based observations of unprecedented quality [13]. The success of SEPIA660 encouraged us to develop a waveguide 2SB mixer for the 800–950 GHz band, which constitutes the next atmospheric window in the sub-mm region. The first 2SB SIS mixer of this design has been manufactured and characterized. In this article, we describe details of the design and subsequently show measurement data from the testing campaign.

II. MIXER DESIGN

For the 2SB mixer, we chose a modular design concept very similar to the one for the 600–720 GHz band [10], [14]. In this concept, the critical components like RF hybrid block, RF horn, local oscillator (LO) horn, and SIS holders "back pieces" are realized as independent units, which can be easily exchanged and tested individually. This allows convenient DSB characterization of the individual SIS devices for matching purposes. A photo of the assembled 2SB mixer block is shown in Fig. 1. Both LO and RF horns have a diagonal spline design described below.

A. RF Waveguide Block

In this section, we present the geometrical design of the key components of the waveguide structure, together with results of numerical simulations. All simulations have been carried out with CST Microwave Studio. The waveguide structure is based on a classical quadrature hybrid architecture, integrated with two LO couplers and an LO splitter into a classical E-plane waveguide split-block [14], shown in Fig. 2. To cover the 800–950 GHz frequency band, a 304×152 μm waveguide was chosen. These dimensions locate the operational band in the high-frequency end of the one-octave single-mode waveguide band in order to minimize waveguide losses. In addition, this ensures compatibility with our mixer back pieces developed earlier for the CHAMP+ instrument [15].

To construct a high performance 2SB receiver, one should pay particular attention to the phase and amplitude balance of
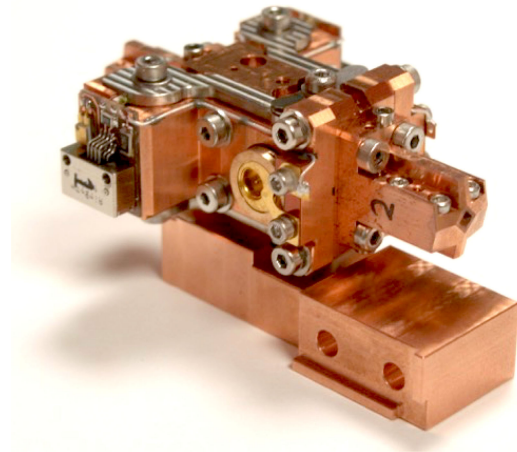

Fig. 1. Photograph of the modular 2SB mixer block. The RF input horn is on the right, the LO horn is on the back opposite to it (not clearly visible). One of back pieces containing one SIS device is visible near the center, with a round GPO connector (Corning Inc., NY, USA) for the IF connection.
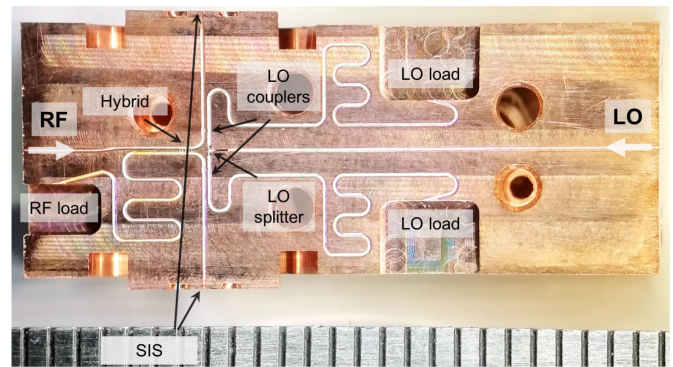

Fig. 2. Photograph of the hybrid block showing the RF waveguide structure. The large white arrows show the inputs for the LO and RF signals. The sign "SIS" indicates the location of the SIS junctions after the backpieces are installed. The scale at the bottom of the photo has a pitch of 1 mm.

the entire RF structure, since RF imbalance is the key parameter limiting the IRR. From our previous work on 2SB SIS mixers for the 650 GHz band [10], [16], [17], we have learned that the total RF balance is strongly influenced by reflections within the RF structure, much more so than by the pure amplitude and phase balance of the RF hybrid itself. Therefore, in addition to the hybrid balance, we have focused on 1) minimizing the hybrid input/output reflections, 2) maximizing the hybrid isolation (directivity), and 3) reducing the RF load reflection. The LO coupler, which is also in the signal path was optimized for low reflection as well.

The waveguides are terminated by large absorber blocks with long waveguides leading up to them (visible in Fig. 2 as meander-shaped structures). The transmission loss of the long waveguides damps out the residual reflections due to mismatches at the waveguide-absorber interfaces. Optionally, these parts of the structure can be coated by a resistive film (e.g., by titanium) to make them even more lossy. Since no strong improvement was found in the past, this was not applied to the mixer presented here.
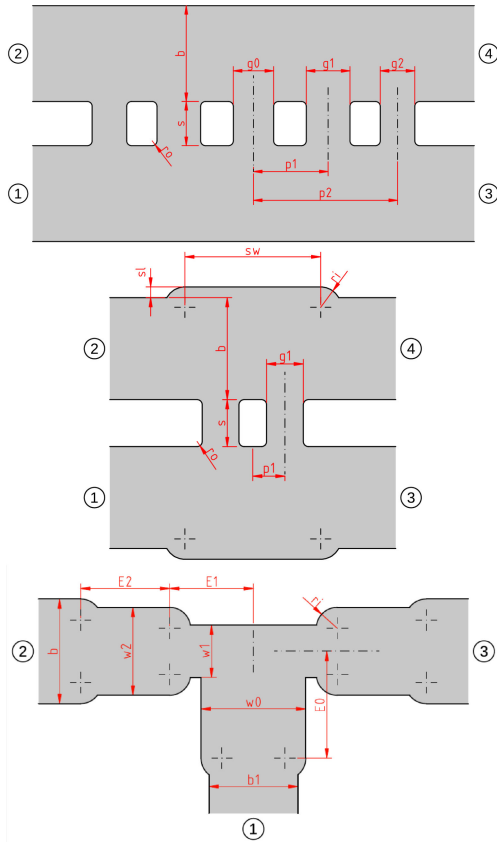
Fig. 3. Layout of the quadrature hybrid (top picture), LO coupler (middle picture) and the LO splitter (bottom picture). The dimensions are shown in Table I. The numbers in circles denote the port numbers as referred to in the text.

TABLE I
DIMENSIONS OF KEY WAVEGUIDE STRUCTURES SHOWN IN FIG. 3

Hybrid		LO coupler		LO split	
Dimension	μm	Dimension	μm	Dimension	μm
b	152	b	152	b	152
s	70	s	70	$b1$	129
$p1$	118	$p1$	48	$w0$	152
$p2$	228	$g1$	55	$w1$	76
$g0$	64	sw	202	$w2$	127
$g1$	69	sl	16	Eo	159
$g2$	55	ri	30	$E1$	121
$r0$	8	$r0$	8	$E2$	129
				ri	30

1) Quadrature Hybrid: The quadrature hybrid (see Fig. 3, top) is a typical five-branch coupler. As mentioned above, the main design goals were the reduction of the input reflection (S_{11}) and the isolation (here labeled S_{21}; the port numbers are indicated in the figure). This was done by optimizing the relevant dimensions (mainly slot widths and positions) while keeping the phase and amplitude balance within reasonable limits (about 0.5° and 0.5 dB, respectively).

Fig. 4 (top plot) shows a representative set of simulated S-parameters. All other S-parameters are identical to one of these four because of symmetry. The gain and phase balance and the total power transmission are presented in the bottom
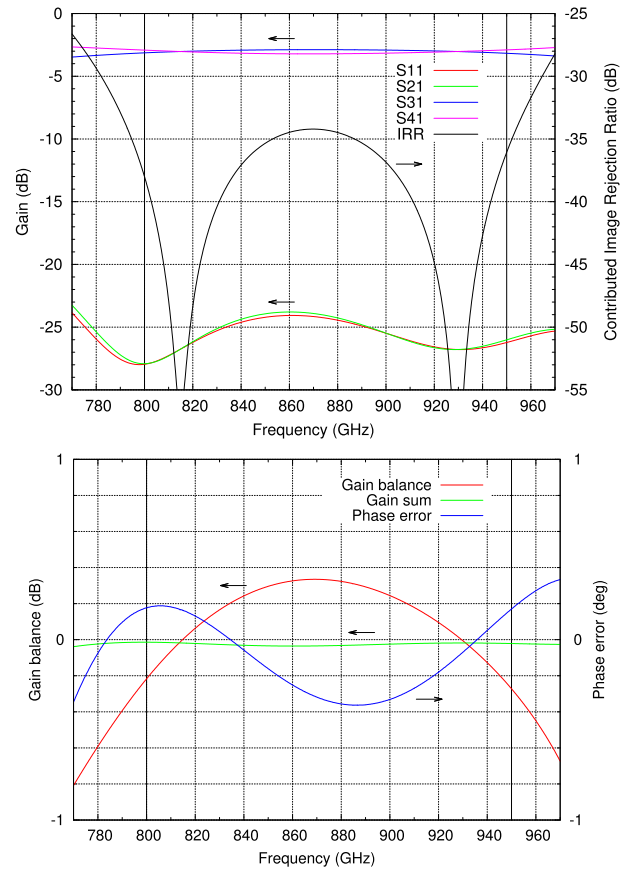

Fig. 4. S-parameters of the simulated hybrid and the hybrid's contribution to the IRR (top plot). Because of symmetry, each of the other S-parameters is identical to one of the four plotted ones. The vertical lines at 800 and 950 GHz indicate the band edges. The bottom plot shows the gain balance $|S_{31}|^2/|S_{41}|^2$, phase error $\arg(S_{31})-\arg(S_{41})-90°$ and the total power throughput "gain sum" $|S_{31}|^2 + |S_{41}|^2$.

plot of the same figure. The crucial input reflection $|S_{11}|^2$ and isolation $|S_{21}|^2$ are both below -24 dB within the band. At the same time, the gain and phase errors are within ±0.4 dB and $\pm0.4°$, respectively. The RF hybrid's contribution to the IRR can be derived from the S-parameters using

$$\text{IRR} = 20 \cdot \log_{10} \frac{|S_{41} + iS_{31}|}{|S_{41} - iS_{31}|}$$

which gives the IRR when all the other components of entire 2SB mixer (including IF hybrid, etc.) are perfect. This is shown on the top plot of Fig. 4 by the curve labeled "IRR." The worst-case point in the band is about -33 dB, which sets the upper limit for the overall image rejection attainable with this design.

2) LO Couplers: The LO is coupled in with a two-branch directional coupler, shown schematically in Fig. 3, middle panel. The design is a scaled version of the LO coupler for the 650 GHz band described in [16]. The simulated S-parameters (not shown here) are virtually identical to ones described there. The coupling factor is set at a level of -13 dB to minimize insertion loss (about 0.25 dB). With the power provided by modern commercial sources (typically several tenths of a milliwatt in this range), this is still more than adequate to pump the SIS mixers optimally.

3) LO Splitter: The LO signal is equally divided between the SIS junctions by an E-plane T-splitter with matching sections in all three branches, as shown in Fig. 3, bottom panel. This splitter is a nondissipative three-port device. As a result, it has both a high reflection in its output ports (S22 and S33) and low isolation between them (S23 and S32). Both impact the LO standing waves in about the same way, therefore, they are chosen to be about equal (≈ -6 dB). The input reflection of the LO input port (S11) was designed to be below -30 dB to avoid problems with standing waves between the RF mixer block and the LO itself.

4) Waveguide Losses: The waveguide length between the RF horn and the SIS junctions (see Fig. 2) is about 12 mm and the waveguide losses should be taken into account, because they directly decrease the 2SB mixer sensitivity. To minimize the resistive losses, a 304×152 μm waveguide was selected, which is close to the maximum possible size for this frequency range while keeping them single-moded. Losses can be estimated using the theory described in [18], but at these frequencies the anomalous skin effect, which happens in metals at low temperature for high-frequency signals [19], [20], should be taken into account. This effect becomes important when the electron mean free path becomes large compared to the classical skin depth, i.e., when standard skin depth model is not longer valid. In case of Cu with a conductivity $\sigma_{300\,\text{K}} = 5.85 \cdot 10^7$ S/m at 300 K and RRR $= 100$, and signals at 870 GHz, the ratio of the mean free path l to the classical skin depth σ is about 0.55 ($l_{300\text{K}} = 38.5$ nm, $\delta_{300\text{K}} = 70.5$ nm) at 300 K [19] and 550 at 4 K ($l_{4K} = 3.85$ μm, $\delta_{4K} = 7$ nm). Consequently, at cryogenic temperatures Cu is deeply in the anomalous skin effect regime in this frequency range, and even close to it at room temperature. Calculation of the loss using the approach from [19], [20] gives 49.5 dB/m at 870 GHz for our waveguide at 4 K. As a result, the loss level for the length of 12 mm is 0.6 dB. This gives about 10% degradation in sensitivity, but keep it profitable to use 2SB mixer instead of DSB one.

The RF blocks were manufactured out of CuTeP alloy (ASTM C14500), which at room temperature has an electrical conductivity similar to that of copper. In the past, we made trials with straight 310×145 μm waveguide extension blocks to measure the resistive loss at around 650 GHz at 4.2 K for different materials. The losses were determined by comparing SIS mixer noise temperatures with and without extension blocks. The results demonstrate similar loss levels of about 50–60 dB/m for both oxygen free Cu (ASTM C10200) and CuTeP alloy [10]. In addition, this number is in good agreement with theoretical calculations, giving 59 dB/m [10], which allows to apply calculations made for pure Cu to the CuTeP alloy.

B. RF and LO Feedhorns

We have designed a smooth-walled spline diagonal split-block horn antenna, as pioneered in [21], to be interfaced to the mixer block. The wall shape is defined by a set of ten nodes, where each node is connected to its nearest neighbors by a straight line (linear spline), as shown in Fig. 5. The nodes have a pair of coordinates, labeled as a_z and a_r, which are the positions along
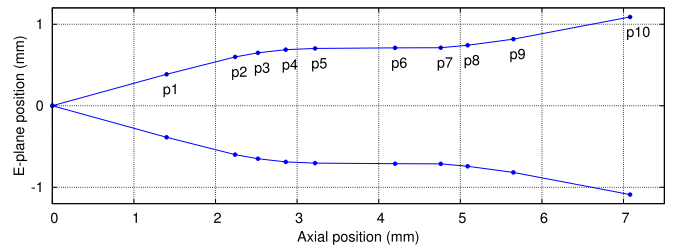

Fig. 5. One-dimenional (1-D) E-plane profile of the smooth-wall diagonal horn antenna. The wall shape is defined by the set of straight lines that connect each node (dots labeled p_i).

TABLE II
PARAMETERS DEFINING THE 1-D WALL PROFILE OF THE HORN ANTENNA

Parameter	a_z(mm)	a_r(mm)
p_1	1.40	0.386
p_2	2.24	0.599
p_3	2.52	0.649
p_4	2.86	0.688
p_5	3.22	0.703
p_6	4.20	0.710
p_7	4.76	0.712
p_8	5.09	0.742
p_9	5.65	0.817
p_{10}	7.08	1.089

the beam propagation axis and the perpendicular axis in the E plane, respectively. The coordinates are listed in Table II. The aperture and length of the horn are defined by the coordinates of the node p_{10}, giving an axial length of 7.08 mm and an aperture of 2.178 mm. The horn is fed using a rectangular (0.304×0.125 mm) waveguide.

Fig. 6 shows the simulated far-field radiation beam pattern of the horn at three key frequencies, 780, 865, and 950 GHz. The simulation shows a very good symmetry between E and H planes down to levels of about -35 dB. This means that the horn will produce a beam with good circular shape or, equivalently, low ellipticity. The sidelobes in both E and H planes are below -40 dB for all the frequencies. Cross-polar levels are below -20 dB at all the frequencies, showing its best performance at 865 GHz. Based on our simulation, we have calculated the beam parameters of this smooth-walled diagonal horn, listed in Table III.

C. SIS Mixers

For this prototype 2SB mixer, we have used SIS mixers devices based on high current density Nb/AlN/NbN tunnel junctions ($J_c = 30$ kA/cm^2) with a microstrip line constructed of a 300 nm thick NbTiN ground plane and a 500-nm-thick Al top layer. The dielectric between the microstrip layers is a 250-nm SiO$_2$ film. On top of the NbTiN bottom layer is deposited a Nb layer, which forms the bottom electrode of the SIS junction, while the NbN top electrode is contacting the Al top layer. More details of the SIS mixer design, fabrication, and characteristics can be found in [15]. A twin SIS junction design was used in this design to provide wideband RF response. The DSB noise
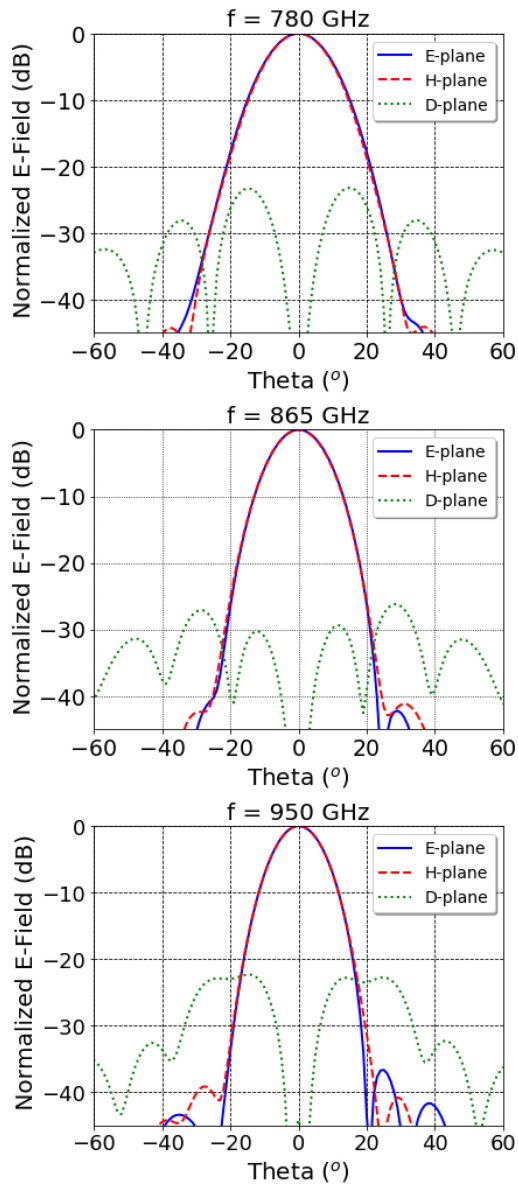
Fig. 6. Simulation results of the far-field radiation beam pattern of the diagonal horn for the bottom, middle, and top of the band. The Co-polar E-field is plotted along cuts in the E and H symmetry planes (solid and dashed lines, respectively), while the cross-polar field is plotted along the diagonal D plane (dotted line), where it is expected to be strongest. The latter is normalized to the maximum copolar signal at the origin.

TABLE III
CALCULATED BEAM PARAMETERS

Freq (GHz)	w_0(mm)	Phase Center (mm)	Beam width (^{o})
780	0.5105	-1.584	13.74
865	0.5143	-0.584	12.29
950	0.5289	-1.484	10.89

temperature of the mixers used to populate our 2SB block is varying from 210 to about 350 K over the band.

D. IF Chain

The two outputs of the RF block each deliver a 4–12 GHz IF signal. They are connected by phase-matched semirigid cables to
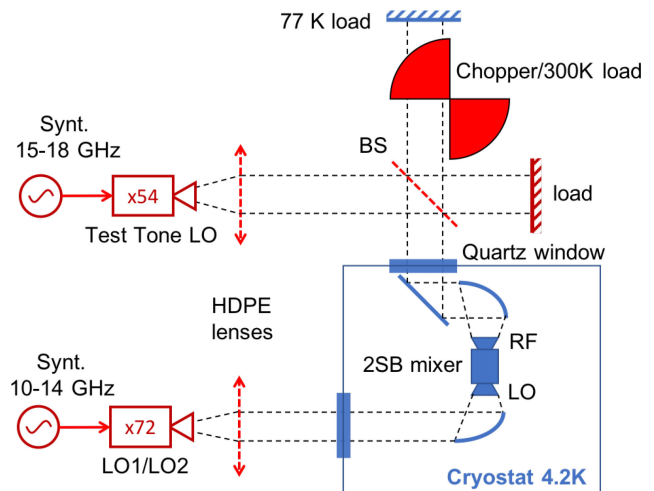

Fig. 7. Scheme of the setup for testing of the 2SB mixer for 850 GHz.

the inputs of a 90° IF hybrid developed by Centro Astronómico de Yebes [22]. This is a state-of-the-art 4–12 GHz cryogenic IF hybrid with an amplitude imbalance below ±0.3 dB, phase imbalance below ±2°, and the isolation (or directivity) and the return losses are below − 22 dB. The further IF chain consists of 4–12 GHz Pamtech isolators and cryogenic amplifiers [23] as used in the ALMA Band nine production receivers [24].

III. RESULTS

The tested RF block and two horns were machined in-house at the Max Plank Institute for Radio Astronomy (MPIfR) in Bonn out of CuTeP (ASTM C14500) alloy. The scheme of the heterodyne test setup is shown in Fig. 7. A liquid He cryostat was used to cool down the mixer. The noise temperature was determined with a 300/77 K hot-cold Y-factor measurement. At the same time, the IRR was characterized according to the method described in [25] by injecting a test tone signal through a 6-μm Mylar beam splitter (6% coupling). Both noise signal and the test tone were coupled to the mixer through a quartz window followed by Gore-Tex infrared filters at 77 and 4 K levels and cold reflective optics. The LO signal is applied through a separate window in the cryostat. Two LO multiplier chains were used, together covering the entire 800–950 GHz band.

A. Noise Temperature

The measured single-sideband (SSB) noise temperature of the prototype mixer is shown in Fig. 8. It varies from about 450–900 K over the band. To enable automated and fast mixer characterization, we left the beam splitter in for the noise temperature measurements and afterward corrected for it. This correction has been verified at two different LO points by separate measurements without the beam splitter. The presented USB and LSB curves are corrected for the fraction of the 300 K noise coupled through the beam splitter and the LO waveguide coupler (4%; − 13 dB in the waveguide LO coupler − 1 dB of additional loss for the 20 mm LO waveguide path, which is calculated using
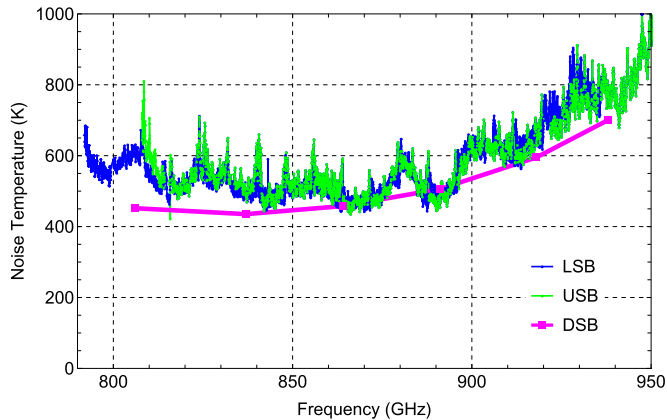
Fig. 8. SSB noise temperature of upper sidebands (USB) and lower sidebands (LSB) as function of the RF input frequency. The SSB noise temperature is corrected for beam splitter and LO couple. The plot is stitched from individual 4–12 GHz IF measurements, while the LO step was 8 GHz, giving full coverage. The frequency resolution within each set is 40 MHz. For reference, the sum of the DSB noise temperatures of the two individual SIS mixer devices is plotted as well (average of two measurements). The DSB noise temperature was measured separately and corrected for a beam splitter used for LO injection. The DSB data points are averaged over the 4–12 GHz IF band, and are plotted versus the LO frequency in this case.

Fig. 9. IRR with the same 2SB mixer block and SIS devices. Both LSB and USB results are presented. The data points are measured with step of 40 MHz.

theoretical estimations given in the previous section. The correction for the LO coupler is applied to have a valid comparison with the DSB mixer noise temperature. In addition, in the future the LO can be located at a much lower temperature stage, which will reduce its noise contribution significantly. To have an estimate of the noise penalty incurred by the waveguide structures, the sum of the DSB noise temperatures of the individual SIS mixers is presented on the same plot. It should be mentioned that the DSB data were obtained using the same cryostat window, cold optics, infrared filters, IF amplifiers, and isolators as for the 2SB measurements. The only difference in optics is that it was measured by injecting the LO signal through a different Mylar beam splitter of 12 μm (12% coupling), but the DSB mixer noise temperature was corrected for this contribution. The contribution of the other optical losses in RF noise is estimated to be below 2 K: 1) the quartz cryostat window has negligible attenuation in this band but a reflection of 5–10%, which gives about 0.5 K contribution from the inner cold surrounding; 2) radiation of the Gore-Tex filters (losses at 700 GHz are known to be about 1.5% [26]) at 77 and 4 K shields is estimated to be 1 K. This contribution is minor and allows reliable estimation of the waveguide losses from the corrected 2SB and DSB noise temperatures.

For clarity, the DSB data points represent the noise temperature averaged over the 4–12 GHz IF band. From the plot, one can estimate that the SSB noise temperature is higher than the DSB one by 0–30% and on average about 15%. This is in a good agreement with the waveguide losses theoretically estimated at 0.6 dB or 15% (see Section II-A4). This is an important conclusion, which confirms a high manufacturing precision of the waveguide structures, high surface quality and low resistivity of the CuTeP material.
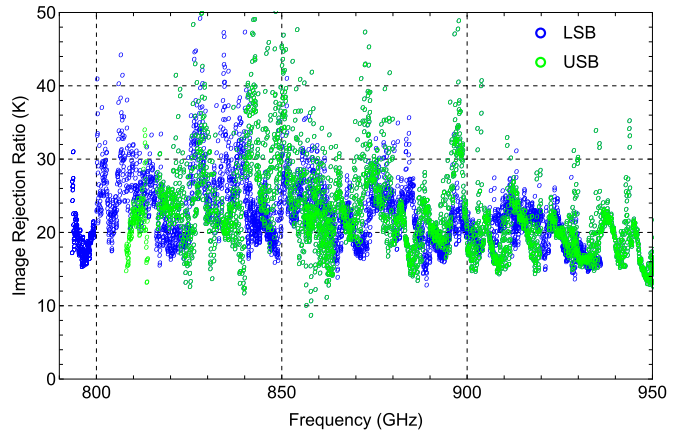
B. Image Rejection

Fig. 9 shows the IRR obtained with the first prototype block. The IRR is above 15 dB in almost all the points, only at the end of the band it goes down to about 13 dB overall. A few points are falling down to 10 dB level, for example, around 860 GHz, which is an artifact of the measurements. It is caused by phase noise and spurious harmonics in the LO signal. Nevertheless, the current results are very promising and a receiver based on this mixer has clear potential to fit ALMA-class specification of 10 dB with ample margin.

IV. CONCLUSION

We designed, manufactured, and tested a new sideband-separating mixer for the 800–950 GHz band. The obtained noise temperatures (450–900 K) can be completely explained by the SIS device noise temperatures and the theoretical losses incurred in the waveguide structure in the anomalous skin-effect regime (about 0.6 dB or 15%). The image rejection is better than 15 dB in most (95%) of the points, and most of the excursions below that (down to about 10 dB) can be attributed to the LO used in the tests. With the current mixers, which are not the best ever demonstrated, the gain in sensitivity for spectral-line observations is about 10% (20% in observation time). If real state-of-the-art SIS devices are employed, the sensitivity gain should go up to about 20% (40% in observation time). It makes the presented waveguide solution an attractive option for potential ALMA upgrades.

REFERENCES

[1] N. Satou *et al.*, "A submillimeter cartridge-type receiver: ALMA Band 8 (385–500 GHz) qualification model," *Publ. Astron. Soc. Jpn*, vol. 60, no. 5, pp. 1199–1207, 2008.

[2] Y. Uzawa *et al.*, "Development and testing of Band 10 receivers for the ALMA project," *Phys. C: Supercond.*, vol. 494, pp. 189–194, 2013.

[3] R. Güsten *et al.*, "APEX: The Atacama Pathfinder Experiment," *Proc. SPIE*, vol. 6267, 2006, Art. no. 626714.

[4] A. Wootten and A. R. Thompson, "The Atacama large millimeter/submillimeter array," *Proc. IEEE*, vol. 97, no. 8, pp. 1463–1471, 2009.

[5] A. Otarola, M. Holdaway, L. E. Nyman, S. J. E. Radford, and B. J. Butler, "Atmospheric transparency at Chajnantor: 1973–2003," in *ALMA Memo Series*, 2005, Memo 512.

[6] [Online]. Available: http://www.apex-telescope.org/weather/, Accessed on: Jun. 15, 2019.

[7] M. Kroug, T. Kojima, Y. Fujii, K. Ohtawara, A. Miyachi, and Y. Uzawa, "Noise performance of ALMA band 10 receivers employing high-jc SIS mixers," in *Proc. 29th IEEE Int. Symp. Space THz Technol.*, Pasadena, CA, USA, 2018.

[8] M. Kroug, "Superconducting mixer technology at NAOJ," in *Proc. ALMA Development Workshop*, Garching, Germany, 2019.

[9] A. R. Thompson and L. R. D'Addario, "Relative sensitivity of double-and single-sideband systems for both total power and interferometry," *ALMA Memo*, vol. 304, 2000.

[10] A. Khudchenko, R. Hesper, A. M. Baryshev, J. Barkhof, and F. P. Mena, "Modular 2SB SIS receiver for 600–720 GHz: Performance and characterization methods," *IEEE Trans. Terahertz Sci. Technol.*, vol. 7, no. 1, pp. 2–9, Jan. 2017.

[11] Y. Fujii *et al.*, "Low-noise integrated balanced SIS mixer for 787–950 GHz," *Supercond. Sci. Technol.*, vol. 30, no. 2, 2016, Art. no. 024001.

[12] R. Hesper *et al.*, "A deployable 600–720 GHz ALMA-type sideband-separating receiver cartridge," in *Proc. 29th Int. Symp. Space Terahertz Technol.*, Pasadena, CA, USA, 2018.

[13] F. M. Montenegro-Montes *et al.*, "Orion-KL observations with the extended tuning range of the new SEPIA660 APEX facility instrument," *Signal*, vol. 581, no. 585, pp. 583–587, 2019.

[14] R. Hesper, G. Gerlofsma, F. P. Mena, M. C. Spaans, and A. M. Baryshev, "A sideband-separating mixer upgrade for ALMA band 9," in *Proc. 12th Int. Symp. Space Terahertz Technol.*, 2009, pp. 257–260.

[15] A. Khudchenko *et al.*, "High-gap Nb-AlN-NbN SIS junctions for frequency band 790–950 GHz," *IEEE Trans. Terahertz Sci. Technol.*, vol. 6, no. 1, pp. 127–132, 1 Jan. 2016.

[16] R. Hesper, A. Khudchenko, A. M. Baryshev, J. Barkhof, and F. P. Mena, "A new high-performance sideband-separating mixer for 650 GHz," in *Proc. Soc. Photo-Opt. Instrum. Eng. Conf. Ser.*, 2016, vol. 9914, pp. 99 140G–1–99 140G–11.

[17] R. Hesper, A. Khudchenko, A. M. Baryshev, J. Barkhof., and F. P. Mena, "A high-performance 650-GHz sideband-separating mixer – design and results," *IEEE Trans. Terahertz Sci. Technol.*, vol. 7, no. 6, pp. 686–693, Nov. 2017.

[18] E. Maxwell, "Conductivity of metallic surfaces at microwave frequencies," *J. Appl. Phys.*, vol. 18, no. 7, pp. 629–638, 1947.

[19] R. Finger and A. R. Kerr, "Microwave loss reduction in cryogenically cooled conductors," *Int. J. Infrared Millimeter Waves*, vol. 29, no. 10, pp. 924–932, 2008.

[20] A. B. Pippard, "The surface impedance of superconductors and normal metals at high frequencies. II. The anomalous skin effect in normal metals," *Proc. Roy. Soc.*, vol. A191, 1947, Art. no. 385.

[21] H. J. Gibson *et al.*, "A novel spline-profile diagonal horn suitable for integration into THz split-block components," *IEEE Trans. Terahertz Sci. Technol.*, vol. 7, no. 6, pp. 657–663, Nov. 2017.

[22] I. Malo-Gómez, J. D. Gallego-Puyol, C. Diez-González, I. López-Fernández, and C. Briso-Rodríguez, "Cryogenic hybrid coupler for ultra-low-noise radio astronomy balanced amplifiers," *IEEE Trans. Microw. Theory Techn.*, vol. 57, no. 12, pp. 3239–3245, Dec. 2009.

[23] I. López-Fernández, J. D. Gallego Puyol, C. D. González, and A. B. Cancio, "Development of cryogenic IF low-noise 4-12 GHz amplifiers for ALMA radio astronomy receivers," in *Proc. IEEE MTT-S Int. Microw. Symp. Dig.*, 2006, pp. 1907–1910.

[24] A. M. Baryshev *et al.*, "The ALMA band 9 receiver - design, construction, characterization, and first light," *A&A*, vol. 577, 2015, Art. no. A129.

[25] A. R. Kerr, S.-K. Pan, and J. E. Effland, "Sideband calibration of millimeter-wave receivers," in *ALMA Memo Series*, 2001, Memo 357.

[26] A. M. Baryshev, M. Candotti, and N. A. Trappe, "Cross-polarization characterization of GORE-TEX slabs at band 9 frequencies," *NRAO, Charlottesville, VA, ALMA Memo*, vol. 551, 2006.

Andrey Khudchenko received the M.S. degree in applied physics and mathematics and the Ph.D. degree in radiophysics from the Moscow Institute of Physics and Technology, Moscow, Russia, in 2007 and 2009, respectively.

From 2004 to 2008, he was an Engineer and, in 2009, a Researcher with the Kotel'nikov Institute of Radio Engineering and Electronics, Russian Academy of Sciences, Moscow, Russia. From 2009 to 2015, he has been an Instrument Scientist with The Netherlands Institute for Space Research SRON, Utrecht, The Netherlands. Since 2015, he has been an Instrument Scientist with the Kapteyn Astronomical Institute, University of Groningen, Groningen, The Netherlands working on the development of new heterodyne THz instruments. It includes development of sideband-separating receiver for the ALMA band 9 (SEPIA660 instrument), CHAMP+ high mixers for the APEX telescope, and work on stabilization of quantum cascade lasers for hot electron bolometer receivers.

Ronald Hesper received the M.Sc. degree from the University of Leiden, Leiden, The Netherlands, in 1994, and the Ph.D. degree from the University of Groningen, Groningen, The Netherlands, in 2000, both in experimental solid state physics.

Since 2000, he has been an Instrument Scientist with the Kapteyn Astronomical Institute, University of Groningen, Groningen, The Netherlands. From 2000 to 2008, he was involved with the technological development of the ALMA Band 9 receivers, including the process of industrialization, as well as related projects like the CHAMP+ mixer arrays for APEX; from 2008 to 2013, on the development of a sideband-separating mixer upgrade for the ALMA Band 9 receivers; and from 2013 to the beginning of 2015, on the industrialization of the ALMA Band 5 receivers. He is currently involved in the development of new (arrayable) heterodyne detector technologies at frequencies around 1 THz.

Andrey M. Baryshev received the master's *(summa cum laude)* degree in physical quantum electronics from the Moscow Institute of Physics and Technology, Moscow, Russia, in 1993, and the Ph.D. degree in THz SIS receivers from the Technical University of Delft, Delft, The Netherlands, in 2005.

He is currently a Senior Instrument Scientist. Since 1998, he has been with the SRON Low Energy Astrophysics Division and the Kapteyn Astronomical Institute, University of Groningen, Groningen, The Netherlands. Since 2000, he has been involved in a joint effort to develop the SIS receiver (600–720 GHz) for ALMA. In 2013, he became an Associate Professor of astronomical instrumentation for the far-infrared with the Kapteyn Astronomical Institute, University of Groningen. His research interests include the areas of heterodyne and direct detectors for large focal plane arrays at THz frequencies, and quasi-optical system design and experimental verification.

Dr. Baryshev was the recipient of a Netherlands Organisation for Scientific Research-VENI grant for research on heterodyne focal plane array technology in 2008, and an EU commission Starting Researcher Grant for work on direct detector focal plane arrays in 2009.

Jan Barkhof received the M.Sc. degree in applied physics from the University of Groningen, Groningen, The Netherlands, in 1999.

From 1999 to 2004, he was an Optical Researcher with Pfizer, where he was involved with an accommodating intra-ocular lens. Since 2004, he has been a Test Engineer with the Kapteyn Astronomical Institute, University of Groningen, developing test systems and software for verifying the quality of ALMA Band 9 and Band 5 receivers.

Kirill Rudakov received the B.S. and M.S. degrees in applied physics and mathematics from the Moscow Institute of Physics and Technology, Moscow, Russia, in 2013 and 2015, respectively. In 2016, he started a Ph.D. research with the Kapteyn Astronomical Institute, Groningen, The Netherlands.

Since 2012, he has been with the Kotel'nikov Institute of Radio Engineering and Electronics of the Russian Academy of Sciences, Moscow, Russia. After internships as a Research Student with the AL-PHA experiment at CERN in 2013 and as a Guest Scientist with the CHAMP+ experiment at a SRON in 2014. There he focused on heterodyne waveguide SIS-based receivers and superconducting circuits HF calculations, and measurements of the.

Michael Fominsky received the M.S. degree from the Moscow Institute of Physics and Technology, Moscow, Russia, in 2000, and the Ph.D. degree from the Kotel'nikov Institute of Radio Engineering and Electronics, Russian Academy of Sciences, Moscow, Russia, in 2011, both in material science.

He is currently a Senior Researcher with the Kotel'nikov Institute of Radio Engineering and Electronics, Russian Academy of Sciences, Moscow, Russia. His research interests include development and fabrication of superconducting circuits and e-beam lithography.

Daniel Montofré received the Degree in physics engineering from the Universidad de Santiago de Chile, Santiago, Chile, in 2014. He is currently working toward the double Ph.D. degree in electrical engineering and astronomy from the Universidad Chile, Santiago, Chile, and the University of Groningen, Groningen, The Netherlands.

His research interests include the development of horn antennas for millimeter/submillimeter astronomical instrumentation, design of frequency selective filters, and quasi-optical design for dual-band observations.

Christopher Heiter received the M.Sc. degree in astroparticle physics from RWTH Aachen University, Aachen, Germany, in 2016. In 2018, he started a Ph.D. research at the same institute, focusing on the design and development of a multi band heterodyne receiver system for the APEX telescope.

From 2016 to 2018, he was an Instrument Scientist for the submm technology division with the Max Planck Institute for Radio Astronomy, Bonn, Germany, where he contributed i.a. to the commissioning of the LASMA receiver at the APEX telescope and the maintenance of the existing receivers.

Duc van Nguyen, photograph and biography not available at the time of publication.

Stefan Heyminck, photograph and biography not available at the time of publication.

Valery P. Koshelets received the M.S. degree in physics from Lomonosov Moscow State University, Moscow, Russia, in 1973, and the Ph.D. degree in radio physics and Doctor of Sciences (Habilitation) degree in physical electronics from the Kotel'nikov Institute of Radio Engineering and Electronics of the Russian Academy of Sciences, Moscow, Russia, in 1978 and 1990, respectively.

Since 1973, he has been with the Kotel'nikov Institute of Radio Engineering and Electronics of the Russian Academy of Sciences, Moscow, Russia, where he is currently the Head of the Laboratory of superconducting devices for signal detection and processing.

Rolf Güsten, photograph and biography not available at the time of publication.

Bernd Klein received the B.Eng. degree in electronics from the University of Applied Science Friedberg, Friedberg, Germany, in 1993, and the M.Eng. degree in theoretical electrical engineering from the University Siegen, Siegen, Germany, in 1996, and the Ph.D. degree in astronomy from the University Bonn, Bonn, Germany, in 2005.

From 1999, he was an Engineer and, from 2002 to 2009, the Head of the laboratory for digital technology with the Max Planck Institute for Radio Astronomy (MPIfR) in Bonn, Germany. In 2009, he became a Professor of digital signal processing and radioastronomical instrumentation with the University of Applied Sciences Bonn-Rhein-Sieg (H-BRS).

Since September 2018, he has been additionally taken over the management of the submm technology division at the MPIfR and since October 2018, he is also CoPI of GREAT at SOFIA.

Pavel N. Dmitriev received the M.S. degree in material science from Lomonosov Moscow State University of Fine Chemical Technologies, Moscow, Russia, in 1993, and the Ph.D. degree in development of SIS mixers from the Kotel'nikov Institute of Radio Engineering and Electronics of the Russian Academy of Sciences, Moscow, Russia, in 1993.

He is currently a Researcher with the Kotel'nikov Institute of Radio Engineering and Electronics of the Russian Academy of Sciences, Moscow, Russia. His research interests include development and fabrication of superconducting circuits.